Hindawi Publishing Corporation
International Journal of Corrosion
Volume 2014, Article ID 356752, 6 pages
http://dx.doi.org/10.1155/2014/356752

Research Article

Electrochemical Investigation of Corrosion Behavior Heat Treated Al-6Si-0.5Mg-xCu ($x = 0$, 0.5, 1, 2, and 4 wt%) Alloys

A. Hossain, F. Gulshan, and A. S. W. Kurny

Department of Materials and Metallurgical Engineering, Bangladesh University of Engineering and Technology, Dhaka 1000, Bangladesh

Correspondence should be addressed to A. Hossain; ahbuetmmesgfl@gmail.com

Received 19 June 2014; Revised 16 November 2014; Accepted 17 November 2014; Published 7 December 2014

Academic Editor: Ramazan Solmaz

The corrosion behaviour of heat treated Al-6Si-0.5Mg-xCu (x = 0.5, 1, 2, and 4 wt%) alloys in 0.1 M NaCl solution was investigated using potentiodynamic polarization and electrochemical impedance spectroscopy (EIS) techniques. The potentiodynamic polarization curves reveal that 2 wt% Cu (Alloy-4) and 4 wt% Cu (Alloy-5) content alloys are more prone to corrosion than the other alloys investigated. But the EIS test results showed that charge transfer resistance (R_{ct}) increases with increasing Cu content into Al-6Si-0.5Mg. Maximum charge transfer resistance (R_{ct}) is reported with the addition of 2 wt% Cu and minimum R_{ct} value is for 4 wt% Cu content Al-6Si-0.5Mg alloy. Due to additions of Cu into Al-6Si-0.5Mg alloy, the magnitudes of open circuit potential (OCP), corrosion potential (E_{corr}), and pitting corrosion potential (E_{pit}) in NaCl solution were shifted to the more noble direction.

1. Introduction

Aluminium and its alloys are considered to be highly corrosion resistant under the majority of service conditions [1]. The various grades of pure aluminium are the most resistant, followed closely by the Al-Mg and Al-Mn alloys. Next in order is Al-Mg-Si and then Al-Si alloy. The alloy containing copper is the least resistant to corrosion; but this can be improved by coating each side of the copper containing alloy with a thin layer of high purity aluminium, thus gaining a three-ply metal, that is, Alclad. This cladding acts as a mechanical shield and also protects the material by sacrificing itself [2]. When aluminium surface is exposed to atmosphere, a thin invisible oxide (Al_2O_3) skin forms, which protects the metal from corrosion in many environments [1]. This film protects the metal from further oxidation unless this coating is destroyed; the material remains fully protected against corrosion [3, 4]. The composition of an alloy and its thermal treatment are of important for susceptibility of alloys to corrosion [5, 6].

Over the years, a number of studies have been carried out to assess the effect of Cu content and the distribution of second phase intermetallic particles on the corrosion behavior of Al-alloys. The Cu distribution in the microstructure affects the susceptibility to localized corrosion. Pitting corrosion usually occurs in the Al-matrix near Cu containing intermetallic particles owing to galvanic interaction with Al-matrix. Intergranular corrosion (IGC) is generally believed to be associated with Cu containing grain boundary precipitates and the precipitate free zone (PFZ) along grain boundaries [7–9]. In heat treatable Al-Si-Mg(-Cu) series alloys, it was found that the susceptibility to localized corrosion (pitting and/or intergranular (IGC)) and the extent of attack are mainly controlled by the type, amount, and distribution of the precipitates which form in the alloy during any thermal or thermomechanical treatments performed during manufacturing processes [10–14].

Depending on the composition of the alloy and parameters of the heat treatment process, these precipitates form in the grain boundaries, or in the bulk as well as grain boundaries. As indicated by several authors, the precipitates formed by heat treatment in Al-Si-Mg alloys containing Cu are the θ (Al_2Cu), Q-phase ($Al_4Mg_8Si_7Cu_2$), β-phase (Mg_2Si), and free Si if Si content in the alloy exceeds the Mg_2Si stoichiometry [15–18].

To understand the corrosion behaviour, different Cu containing (0.5, 1, 2, and 4 wt%) Al-6Si-0.5Mg alloys were tested using electrochemical methods in 0.1 M NaCl solution.

Table 1: Impedance test results.

Alloy code	Alloy compositions	R_s (Ω)	R_{ct} (kΩ)	C_{dl} (μF)	OCP (V/SEC)
Alloy-1	Al-6Si-0.5Mg	40.37	15.57	1.259	−0.8454
Alloy-2	Al-6Si-0.5Mg-0.5Cu	43.93	25.75	1.793	−0.7037
Alloy-3	Al-6Si-0.5Mg-Cu	44.08	27.13	3.219	−0.6534
Alloy-4	Al-6Si-0.5Mg-2Cu	50.93	28.33	2.012	−0.6574
Alloy-5	Al-6Si-0.5Mg-4Cu	47.97	6.435	2.942	−0.6263

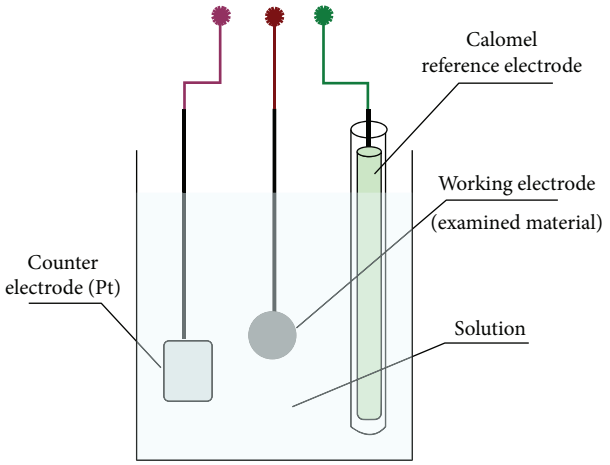

Figure 1: Schematic representation of the three-electrode system cell.

The corroded surfaces of alloys were examined after exposure using a scanning electron microscope (SEM) to understand better the corrosion mechanisms.

2. Materials and Methods

2.1. Materials Preparation. The Al-6Si-0.5Mg-xCu (x = 0.5, 1, 2, and 4 wt%) alloys were prepared by melting Al-7Si-0.3Mg (A356) alloys and adding Cu into the melt. The melting operation was carried out in a gas fired clay-graphite crucible furnace and the alloys were cast in a permanent steel mould. After solidification of alloys, rectangular samples (30 mm × 10 mm × 5 mm) were cut. The samples were homogenised (500°C for 24 hr) and solutionized (540°C for 2 hr) and finally artificially aged (225°C for 1 hr). After heat treatment the rectangular samples (30 mm × 10 mm × 5 mm) were prepared for metallographical observation and finally subjected to electrochemical test. Deionized water and analytical reagent grade sodium chloride (NaCl) were used for the preparation of 0.1 M solution. All measurements were carried out at room temperature.

2.2. Electrochemical Measurements

2.2.1. Potentiodynamic Polarization Measurements. A computer-controlled Gamry Framework TM Series G 300 and Series G 750 Potentiostat/Galvanostat/ZRA were used for the electrochemical measurements. The potentiodynamic polarization studies were configured in cells (Figure 1), using three-electrode assembly with a saturated calomel reference electrode, a platinum counter electrode, and the sample as working electrode in the form of coupons of exposed area of 0.50 cm^2 or 10 mm × 5 mm. Only one 10 mm × 5 mm surface area was exposed to the test solution and the other surfaces were covered with Teflon tape and allowed to establish a steady state open circuit potential (OCP). The potential range selected was −1 to +1 V and measurements were made at a scan rate of 0.50 mV/s. First 100s applied for achieving steady state OCP and for potential −1 V to +1 V immersion time was about 67 minutes. The corrosion current (I_{corr}, measured by Butler-Volmer equation), corrosion potential (E_{corr}), pitting corrosion potential (E_{pit}), and corrosion rate (mpy) were calculated from Tafel curve. The tests were carried out at room temperature in solutions containing 0.1 M of NaCl at a fixed and neutral pH value. No stirring was applied and the experiments were carried out in a closed cell. The corroded samples were cleaned in distilled water and examined under a scanning electron microscope.

2.2.2. Electrochemical Impedance Measurements. As in potentiodynamic polarization tests, three-electrode cell arrangement was also used in electrochemical impedance measurements. Rectangular samples (10 mm × 5 mm) were connected with copper wire and adopted as working electrodes for impedance measurements. EIS tests were performed in 0.1 M NaCl solution at room temperature over a frequency range of 100 kHz to 0.2 Hz using a 5 mV amplitude sinusoidal voltage. The 10 mm × 5 mm sample surface was immersed in 0.1 M NaCl solution (corrosion medium). All the measurements were performed at the open circuit potential (OCP). The test cells were maintained at room temperature and the NaCl solution was refreshed regularly during the whole test period. The impedance spectra were collected, and the experimental results were fitted to an equivalent circuit (EC) using the Echem Analyst data analysis software. The solution resistance (R_s), polarization resistance, or charge transfer resistance (R_{ct}) and double layer capacitance (C_{dl}) of the thermal treated alloys were determined.

3. Results and Discussion

3.1. Impedance Measurements. Table 1 shows the electrochemical impedance spectroscopy (EIS) results obtained from the electrochemical tests.

OCP versus Time Behavior. Large fluctuations in open circuit potential for the peak aged Al-6Si-0.5Mg-xCu alloys in 0.1 M

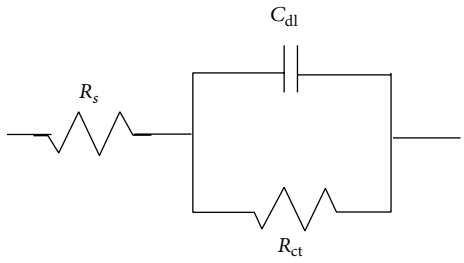

Figure 2: Electrical equivalent circuit used for fitting of the impedance data of alloys in 0.1 M NaCl solution.

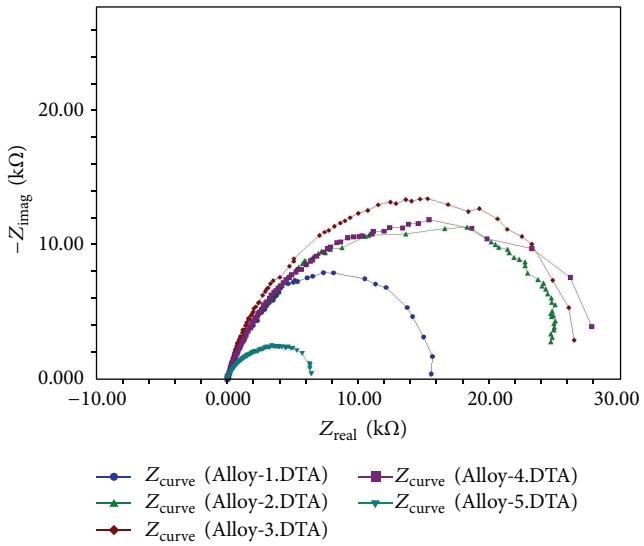

Figure 3: Nyquist plot for the aged alloys 1–5 in 0.1 M NaCl solution.

NaCl solution were seen (Table 1) during the time of 100s exposure. Afterwards the OCP fluctuation decreased and reached about steady state. The steady state OCP of Cu free alloy (Alloy-1) is −0.8454 V and it is the most negative potential compared to the OCP value of other Cu content alloys. The occurrence of a positive shift in the OCP of Al-6Si-0.5Mg alloys containing 0.5–4 wt% Cu indicates the existence of anodically controlled reaction. The OCP values mainly depend on the chemical compositions of the alloys.

The data obtained were modeled and the equivalent circuit that best fitted the results is shown in Figure 2. Rs represents the ohmic resistance of the electrolyte. R_{ct} and C_{dl} are the charge transfer resistance and electrical double layer capacitance, respectively, which correspond to the Faradaic process at the alloy/media interface. Figure 3 shows the Nyquist diagrams of the Al-6Si-0.5Mg-xCu alloys in 0.1 M NaCl solution. Nyquist curves with suggested equivalent circuit model for the different Cu content in 0.1 M NaCl solution is shown in Figure 3. In Nyquist diagrams, the imaginary component of the impedance (Z'') against real part (Z') is obtained in the form of capacitive-resistive semicircle for each sample.

The solution resistance of the alloys varies from 40 to 51 Ω and the R_s values of the alloys are very similar to each other.

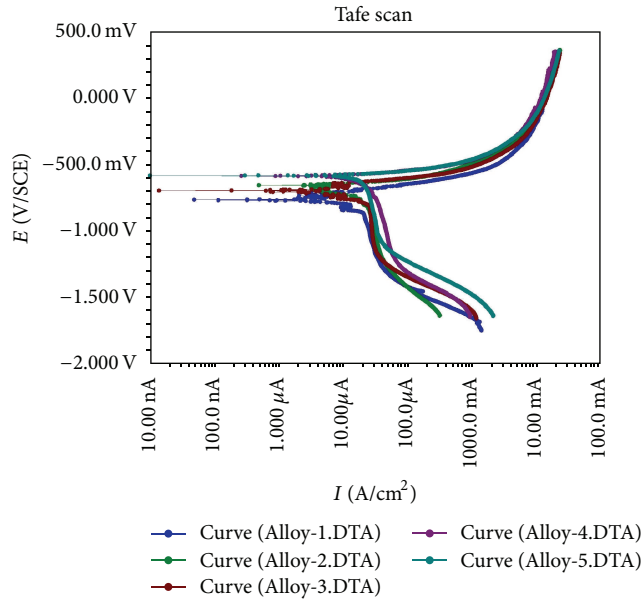

Figure 4: Potentiodynamic polarization curves of aged alloys 1–5 in 0.1 M NaCl solution.

So there are insignificant changes in R_s values for the alloys during EIS testing. Impedance measurements showed that, in 0.1 M NaCl solution, increasing Cu in the Al-6Si-0.5Mg alloys increases the charge transfer resistance. For the Cu free Al-6Si-0.5Mg alloy (Alloy-1), the charge transfer resistance (R_{ct}) value in 0.1 M NaCl solution is 15.57 kΩ, and this is increased to 28.33 kΩ with addition of 2 wt% Cu to the Al-6Si-0.5Mg alloy (Alloy-4). These increases in the charge transfer resistance show the increase in the corrosion resistance of the alloys with Cu addition. The Al-6Si-0.5Mg alloy shows a maximum charge transfer resistance at 2 wt% Cu. Further addition of Cu (4 wt% in Alloy-5) causes a dramatical drop in the corrosion resistance of the Al-6Si-0.5Mg alloy because of the overalloying and excessive intermetallic particles. The Al-6Si-0.5Mg-4Cu alloy (Alloy-5) shows the lowest charge transfer resistance (6.435 kΩ) among the investigated alloys. The double layer capacitance (C_{dl}) of the Cu free Al-6Si-0.5Mg alloy (Alloy-1) is 1.259 μF, which is the lowest value among the investigated alloys, and it increased with the additions of Cu and the maximum was found for Alloy-3.

3.2. Potentiodynamic Polarization Measurements. Table 2 shows the potentiodynamic polarization test results obtained from the electrochemical tests.

Potentiodynamic polarization curves of Al-6Si-0.5Mg-xCu alloys in 0.1 M NaCl solution are shown in Figure 4. Anodic current density of Al-6Si-0.5Mg-xCu alloys decreased with Cu addition. This decrement is caused by slowing of the anodic reaction of Al-6Si-0.5Mg-xCu alloy due to the addition of Cu and microgalvanic cells caused in α-aluminum matrix. Different intermetallic compounds, like Mg_2Si, Al_2Cu, and so forth, can form microgalvanic cells because of the difference of corrosion potential between intermetallics and α-aluminum matrix. The electrochemical

Table 2: Potentiodynamic polarization test results.

Alloy code	I_{corr} (μA/cm^2)	E_{corr} (mV)	E_{pit} (mV)	Corrosion rate (mpy)
Alloy-1	6.300	−764	−480	5.287
Alloy-2	5.640	−657	−408	4.732
Alloy-3	2.950	−697	−370	2.474
Alloy-4	20.30	−586	−353	17.050
Alloy-5	16.30	−583	−340	13.650

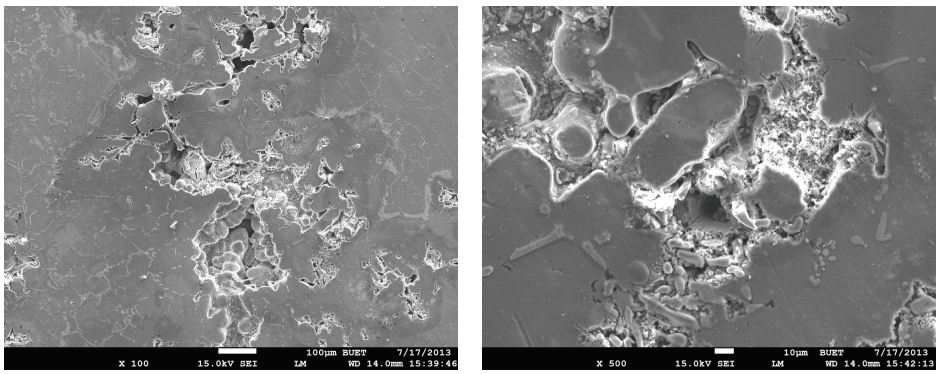

Figure 5: SEM secondary electron image of the damage surface morphology of as-corroded T6 peak aged Al-6Si-0.5Mg alloy (Alloy-1) in 0.1 M NaCl solution. Microstructures at different magnifications indicate severe pits deeper and wider than that observed in Figures 7 and 8.

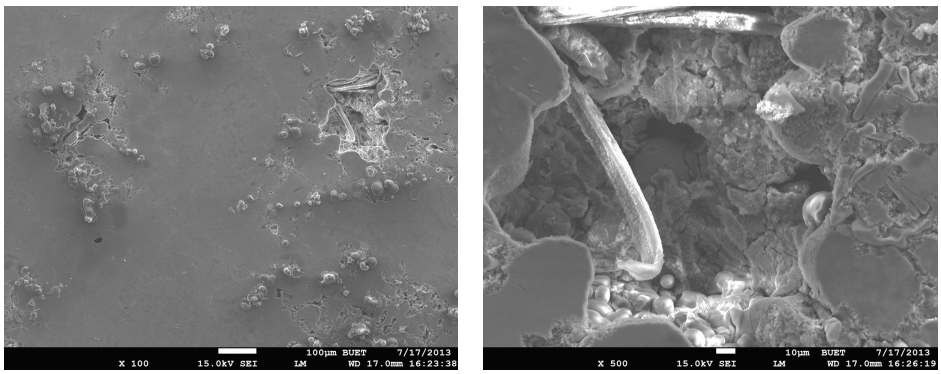

Figure 6: SEM secondary electron image of the damage surface morphology of as-corroded T6 peak aged Al-6Si-0.5Mg-0.5Cu alloy (Alloy-2) in 0.1 M NaCl solution. Microstructures at different magnifications indicate severe pits deeper and wider than that observed in Figure 7.

parameters (I_{corr}, E_{corr}, E_{pit}, and corrosion rate) obtained from potentiodynamic polarization curves were presented in Table 2. The corrosion potential (E_{corr}) value increased with increasing of Cu content to Al-6Si-0.5Mg alloy. In the Cu free Al-6Si-0.5Mg alloy (Alloy-1), corrosion potential is −764 mV, which is the highest negative potential among the investigated alloys. With increasing Cu, corrosion potential of the alloys were shifted towards more positive values and 4 wt% Cu alloy (Alloy-4) has the lowest potential (−583 mV) in these alloys. Pitting potential of all alloys also shifted more positive values according to corrosion potential. The pitting potential varied from −480 mV to −353 mV. The I_{corr} value of Cu free Al-6Si-0.5Mg alloy (Alloy-1) is 6.3 μA/cm^2 and corrosion rate is 5.287 mpy. The current density (I_{corr}) values decrease for 0.5 and 1 wt% Cu content alloys (Alloy-2 = 5.640 μA/cm^2 and Alloy-3 = 2.950 μA/cm^2). And the corresponding corrosion rate decreases for these alloys (Alloy-2 = 4.732 mpy and Alloy-3 = 2.474 mpy). But in the case of 2 and 4 wt% Cu content alloys (Alloy-4 and Alloy-5) current density (20.30 μA/cm^2 and 16.30 μA/cm^2) tremendously increased and the corresponded corrosion rates (17.05 mpy and 13.65 mpy) are also increased.

3.3. Microstructural Investigation. The microstructure of selected as-corroded samples using SEM indicates pronounced pits showing that the samples have suffered pitting corrosion attack. The exposed surface shows evidence of localized attack at the location of the Intermetallics caused by the dissolution of the matrix. There was evidence of corrosion products in all the samples examined. It is provable that the pits are formed by intermetallic dropping out from the surface due to the dissolution of the surrounding matrix.

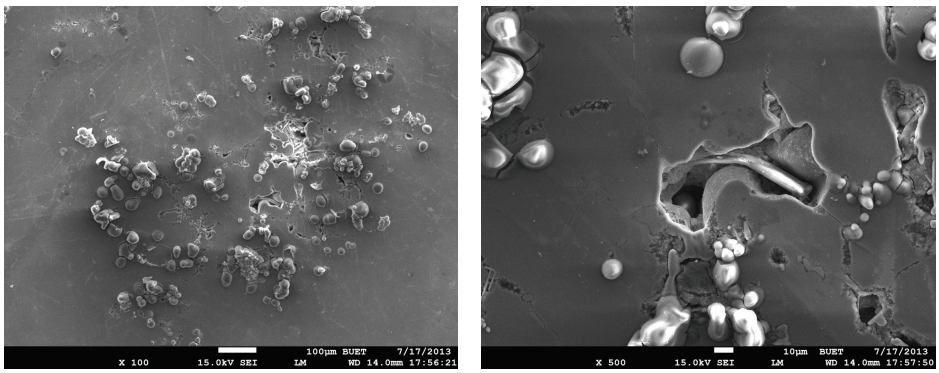

Figure 7: SEM secondary electron image of the damage surface morphology of as-corroded T6 peak aged Al-6Si-0.5Mg-Cu alloy (Alloy-3) in 0.1 M NaCl solution. Microstructures at different magnifications indicate several and severe pits.

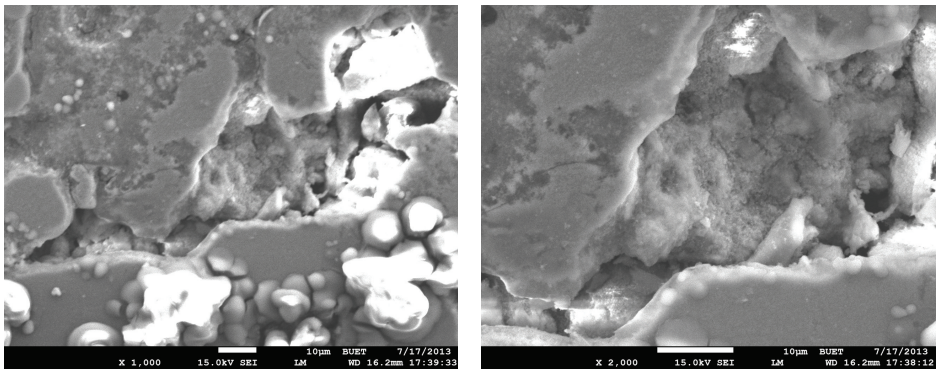

Figure 8: SEM secondary electron image of the damaged surface morphology of as-corroded peak aged Al-6Si-0.5Mg-4Cu alloy (Alloy-5) in 0.1 M NaCl solution. Microstructures at different magnifications indicate severe pits deeper and wider than those observed in Figures 5, 6, and 7.

However, it is also possible that the pits are caused by selective dissolution of the intermetallics/or particles of the second phase precipitates. Consequently, the forms of corrosion in the studied Al-6Si-0.5Mg-*x*Cu alloys are slightly uniform and predominantly pitting as obtained by the SEM.

Samples were characterized by SEM following potentiodynamic polarization tests. The peak aged Cu free alloy (Alloy-1) exhibited pits on their surface, which apparently had nucleated randomly. Conversely, the exposed surface of the alloys exhibited a corrosion product with a rippled appearance covering the surface after polarization. The 4 wt% Cu content peak aged Alloy-5 is more susceptible to pitting corrosion than that of the other alloys (except Alloy-4). Figures 5–8 reveal clearly that pits density of Alloy-5 is much more than that of Cu free alloy (Alloy-1) and 1 wt% Cu content Alloy-3. In Figures 5 and 8, there seems to be uniform surface pits formations which are highly deeper as compared to that in Alloy-3.

4. Conclusions

(1) From the EIS test, the R_{ct} value as an impedance parameter of the alloys shows a maximum at 2 wt% Cu. Further addition of Cu causes a dramatical drop in the charge transfer resistance of Alloy-5 because of the overalloying excess intermetallic phases.

(2) From the linear polarization and Tafel extrapolation plot, the I_{corr} and corrosion rate (mpy) decrease with increasing of Cu content up to 1 wt%. Further addition of Cu (2 and 4 wt%) the I_{corr} values and the corrosion rates are higher among the investigated alloys.

(3) Consequently, the forms of corrosion in the studied Al-6Si-0.5Mg-*x*Cu alloys are uniform pitting corrosion as obtained from the SEM study with pits observations.

Conflict of Interests

The authors declare that there is no conflict of interests regarding the publication of this paper.

Acknowledgment

The authors are thankful to Pilot Plant and Process Development Centre (PP & PDC), BCSIR, Dhaka, Bangladesh, for providing facilities to carry out the electrochemical tests.

References

[1] M. G. Fontana and N. D. Greene, *Corrosion Engineering*, McGraw-Hill Book, New York, NY, USA, 1987.

[2] E. C. Rollason, *Metallurgy for Engineers*, Richard Clay and Company, Bungay, UK, 1964.

[3] S. H. Avner, *Introduction to Physical Metallurgy*, McGraw-Hill, London, UK, 2nd edition, 1974.

[4] G. M. Scamans, J. A. Hunter, and N. J. H. Holroyd, "Corrosion of aluminium—a new approach," in *Proceedings of the 8th International Light Metals Congress*, pp. 699–705, Leoban, Vienna, Austria, 1989.

[5] M. Czechowski, "Effect of anodic polarization on stress corrosion cracking of some aluminium alloy," *Advances in Materials Science*, vol. 7, no. 11, pp. 13–20, 2007.

[6] M. Abdulwahab, I. A. Madugu, S. A. Yaro, and A. P. I. Popoola, "Degradation behavior of high chromium sodium-modified A356.0-type Al-Si-Mg alloy in simulated seawater environment," *Journal of Minerals & Materials Characterization & Engineering*, vol. 10, no. 6, pp. 535–551, 2011.

[7] M. J. Robinson, "Mathematical modelling of exfoliation corrosion in high strength aluminium alloys," *Corrosion Science*, vol. 22, no. 8, pp. 775–790, 1982.

[8] C. S. Paglia, M. C. Carroll, B. C. Pitts, T. Reynolds, and R. G. Buchheit, "Strength, corrosion, and environmentally assisted cracking of a 7075-T6 friction stir weld," *Materials Science Forum*, vol. 396, no. 3, pp. 1677–1684, 2002.

[9] T. Ramgopal, P. I. Gouma, and G. S. Frankel, "Role of grain-boundary precipitates and solute-depleted zone on the intergranular corrosion of aluminum alloy 7150," *Corrosion*, vol. 58, no. 8, pp. 687–697, 2002.

[10] G. Svenningsen, M. H. Larsen, J. H. Nordlien, and K. Nisancioglu, "Effect of high temperature heat treatment on intergranular corrosion of AlMgSi(Cu) model alloy," *Corrosion Science*, vol. 48, no. 1, pp. 258–272, 2006.

[11] G. Svenningsen, M. H. Larsen, J. C. Walmsley, J. H. Nordlien, and K. Nisancioglu, "Effect of artificial aging on intergranular corrosion of extruded AlMgSi alloy with small Cu content," *Corrosion Science*, vol. 48, no. 6, pp. 1528–1543, 2006.

[12] G. Svenningsen, M. H. Larsen, J. H. Nordlien, and K. Nisancioglu, "Effect of thermomechanical history on intergranular corrosion of extruded AlMgSi(Cu) model alloy," *Corrosion Science*, vol. 48, no. 12, pp. 3969–3987, 2006.

[13] G. Svenningsen, J. E. Lein, A. Bjørgum, J. H. Nordlien, Y. Yu, and K. Nisancioglu, "Effect of low copper content and heat treatment on intergranular corrosion of model AlMgSi alloys," *Corrosion Science*, vol. 48, no. 1, pp. 226–242, 2006.

[14] M. H. Larsen, J. C. Walmsley, O. Lunder, and K. Nisancioglu, "Significance of low copper content on grain boundary nanostructure and intergranular corrosion of AlMgSi(Cu) model alloys," *Materials Science Forum*, vol. 519–521, no. 1, pp. 667–672, 2006.

[15] H. Zhan, J. M. C. Mol, F. Hannour, L. Zhuang, H. Terryn, and J. H. W. de Wit, "The influence of copper content on intergranular corrosion of model AlMgSi(Cu) alloys," *Materials and Corrosion*, vol. 59, no. 8, pp. 670–675, 2008.

[16] M. H. Larsen, J. C. Walmsley, O. Lunder, R. H. Mathiesen, and K. Nisancioglu, "Intergranular corrosion of copper-containing AA6*xxx* AlMgSi aluminum alloys," *Journal of the Electrochemical Society*, vol. 155, no. 11, pp. C550–C556, 2008.

[17] M. H. Larsen, J. C. Walmsley, O. Lunder, and K. Nisancioglu, "Effect of excess silicon and small copper content on intergranular corrosion of 6000-series aluminum alloys," *Journal of the Electrochemical Society*, vol. 157, no. 2, pp. C61–C68, 2010.

[18] S. Zor, M. Zeren, H. Ozkazanc, and E. Karakulak, "Effect of Cu content on the corrosion of Al-Si eutectic alloys in acidic solutions," *Anti-Corrosion Methods and Materials*, vol. 57, no. 4, pp. 185–191, 2010.